Vol. 738: 225–242, 2024
https://doi.org/10.3354/meps14607

MARINE ECOLOGY PROGRESS SERIES
Mar Ecol Prog Ser

Published June 20

Effects of elevated pCO_2 on bioenergetics and disease susceptibility in Pacific herring *Clupea pallasii*

C. S. Murray[1,3,*], J. L. Gregg[2], A. H. Mackenzie[2], H. T. Jayasekera[2], S. Hall[2], T. Klinger[1], P. K. Hershberger[2]

[1]School of Marine and Environmental Affairs and Washington Ocean Acidification Center, University of Washington, Seattle, WA 98105, USA

[2]U.S. Geological Survey, Western Fisheries Research Center, Marrowstone Marine Field Station, Nordland, WA 98358, USA

[3]*Present address:* Biology Department, Woods Hole Oceanographic Institution, Woods Hole, MA 02543, USA

ABSTRACT: Ocean acidification can affect the immune responses of fish, but effects on pathogen susceptibility remain uncertain. Pacific herring *Clupea pallasii* were reared from hatch under 3 CO_2 partial pressure (pCO_2) treatments (ambient, ~650 µatm; intermediate, ~1500 µatm; high, ~3000 µatm) through metamorphosis (98 d) to evaluate the effects of ocean acidification on bioenergetics and susceptibility to an endemic viral disease. Mortality from viral hemorrhagic septicemia (VHS) was comparable between herring reared under ambient and intermediate pCO_2 (all vulnerability testing at ambient pCO_2). By contrast, fish reared under high pCO_2 experienced significantly higher rates of VHS mortality, and the condition factor of survivors was significantly lower than in the other pCO_2 treatments. However, the prevalence of infection among survivors was not influenced by pCO_2 treatment. Pre-flexion larval development was not affected by elevated pCO_2, as growth rate, energy use, and feeding activity were comparable across treatments. Similarly, long-term growth (14 wk) was not affected by chronic exposure to elevated pCO_2. Herring reared under both elevated pCO_2 treatments showed an average reduction in swimming speed; however, wide intra-treatment variability rendered the effect nonsignificant. This study demonstrates that the VHS susceptibility and bioenergetics of larval and post-metamorphic Pacific herring are not affected by near-future ocean acidification predicted for coastal systems of the North Pacific. However, increased susceptibility to VHS in fish reared under 3000 µatm pCO_2 indicates potential health and fitness consequences from extreme acidification.

KEY WORDS: Ocean acidification · Viral hemorrhagic septicemia virus · Immune response · Early life history · Growth · Swimming performance · Forage fish

1. INTRODUCTION

The confluence of anthropogenic climate change and pathogenic disease represents a growing threat to marine biodiversity. Rapidly changing environmental conditions threaten to alter several elements of the host—pathogen—environment relationship, including direct effects on the functional immune response of animal hosts (Burge & Hershberger 2020). Indeed, there is growing evidence that stress-induced immune dysfunction is a driving force behind outbreaks of infectious disease among several marine animal groups (Tracy et al. 2019). Ocean acidification is one of the major consequences of anthropogenic carbon emissions and is driven by the uptake of anthropogenic CO_2 by the oceans. This process is

*Corresponding author: christopher.murray@whoi.edu

Publisher: Inter-Research · www.int-res.com

rapidly altering seawater carbonate chemistry, resulting in a higher partial pressure of CO_2 (pCO_2) and reduced pH (Doney et al. 2020). Acidification in coastal ecosystems is further exacerbated by microbial production of CO_2, which has been amplified by eutrophication and ocean warming (Cai et al. 2021). Biological responses to future pCO_2 conditions have been intensively studied in recent decades, revealing a range of deleterious impacts across a diverse group of marine taxa (Doney et al. 2020). Furthermore, there is mounting evidence that ocean acidification can alter susceptibility to disease in marine invertebrates (Liu et al. 2016, Zha et al. 2017, Cao et al. 2018), raising the possibility that rising ocean pCO_2 will have widespread impacts on pathogen–host interactions (Tangherlini et al. 2021).

Despite this emerging threat, potential impacts on the pathogen resistance of fish have not been adequately studied. This is partially because fish are relatively tolerant of projected changes in ocean pCO_2, given a robust capacity to regulate internal acid–base balance (Ishimatsu et al. 2008). Direct effects on survival are generally limited to the sensitive early life stages of some (Murray et al. 2019, Dahlke et al. 2020, Alter & Peck 2021), but not most (Lonthair et al. 2017, Murray & Baumann 2018, Kwan et al. 2021), experimentally tested species. However, successful acclimation to elevated pCO_2 requires important biochemical and metabolic adjustments that are mediated by broad changes in gene expression (Mittermayer et al. 2019, Schunter et al. 2021). Sublethal effects stemming from the molecular response to elevated pCO_2 are relatively common, including impacts on ion regulation (Kreiss et al. 2015, Michael et al. 2016), energy metabolism and growth (Murray & Baumann 2020, Ruiz-Jarabo et al. 2021), behavior (Williams et al. 2019, Hamilton et al. 2023), and stress responses (Servili et al. 2023). Importantly, ocean acidification may directly impact immune system functionality in fish. Several species have shown modified regulation of immune response genes after exposure to elevated pCO_2, including increased expression of immune factors related to pathogen identification and defense (Bresolin de Souza et al. 2016, Huth & Place 2016, Kang et al. 2022, Toy et al. 2022). In at least one example, long-term multigenerational acclimation of European sea bass *Dicentrarchus labrax* to ocean acidification had a large positive effect on host immunity, resulting in increased resistance to a betanodavirus (Cohen-Rengifo et al. 2022). However, opposing transcriptional responses related to pathogen defense have been observed in different species of coral reef fishes that inhabit the acidified waters near volcanic CO_2 seeps (Kang et al. 2022). Thus, changes in immune function under elevated pCO_2 are probable, but the directionality of the response is likely to be species-specific and depend on the intensity and duration of exposure.

Pacific herring *Clupea pallasii* is a widespread and critically important forage fish species that inhabits coastal marine ecosystems throughout the North Pacific Ocean (Surma et al. 2021). These fish are highly susceptible to viral hemorrhagic septicemia virus (VHSV), a widespread rhabdovirus that causes acute disease (viral hemorrhagic septicemia, VHS) in over 140 Northern Hemisphere fish species (Escobar et al. 2018). Pacific herring is a major reservoir species for VHSV in marine habitats, and infected individuals can become super-spreaders by shedding copious amounts of exogenous virus into the environment, which promotes rapid transmission to conspecifics and other cooccurring species (Hershberger et al. 2021a). The disease has caused recurring epizootics in Pacific herring populations (Hershberger et al. 2021b) and likely contributed to the collapse and failed recovery of the Prince William Sound stocks during the 1990s (Marty et al. 2010). Understanding the environmental variables that influence the progression of VHSV epizootics in Pacific herring remains an important area of active research (Hershberger et al. 2016).

The greater Salish Sea provides critical reproductive habitat for Pacific herring, supporting over 20 distinct spawning populations in US and Canadian waters (Sandell et al. 2019). At the same time, the Salish Sea is highly vulnerable to ocean acidification, as pCO_2 in the Salish Sea is rising faster than the global average due to a combination of anthropogenic and natural factors, including the upwelling and transport of CO_2-enriched ocean waters into coastal systems (Cai et al. 2021). The fitness of some marine ectotherms is already being impacted by seasonal pCO_2 fluctuations in the Salish Sea (McLaskey et al. 2016, Bednaršek et al. 2021), particularly during winter, when pCO_2 regularly exceeds 800 µatm (Evans et al. 2019). Most herring stocks in the region spawn during winter or early spring, and thus offspring development often coincides with peak seasonal acidification in nearshore natal habitats (Pacella et al. 2018). Studies of the CO_2 tolerance of Pacific herring have been limited to the embryonic stage, revealing largely neutral effects of increased pCO_2 on embryonic development, metabolism, and tolerance to heat stress (Murray & Klinger 2022, Singh et al. 2023), but small reductions to embryo survival have been observed (Villalobos et al. 2020). Several studies

have evaluated the effects of elevated pCO_2 on the larvae of Atlantic herring *C. harengus*, with one experiment showing reduced growth and increased rates of tissue damage (Frommel et al. 2014), whereas other research has demonstrated minor effects on growth, survival, and swimming activity (Sswat et al. 2018). Thus, there is a need for longer-term studies focused on Pacific herring that span multiple life stages to better understand the effects on bioenergetics and immunological function.

This study evaluated the effects of ocean acidification on the health, survival, fitness, and disease susceptibility of early life stage Pacific herring. Wild larvae were reared from hatching to determine the effects of elevated pCO_2 on larval growth, yolk consumption, and foraging capabilities and to evaluate how chronic exposure to elevated pCO_2 affects long-term growth and maximum swimming speed. After prolonged exposure (98 d), we tested how elevated pCO_2 experienced during development altered the susceptibility of juvenile Pacific herring to VHS following water-borne exposure to VHSV.

2. MATERIALS AND METHODS

2.1. Animal source

Animal care and experimental procedures were approved by the Institutional Animal Use and Care Committee at the Western Fish Health Science Center (protocol 2008-51). Naturally fertilized Pacific herring embryos were collected from several locations in Port Gamble Bay, WA (USA), on 25 March 2021, by personnel from the Washington Department of Fish and Wildlife and were transported to the US Geological Survey, Marrowstone Marine Field Station (Nordland, WA). Tens of thousands of embryos (developmental stage I; Kawakami et al. 2011) still attached to eelgrass substrate were transferred to an aerated 260 l tank supplied with single-pass, treated (sand-filtered, particle-filtered to 10 µm, and UV-irradiated) seawater from nearby Admiralty Inlet maintained at ambient temperature (~8.5°C), salinity (~30‰), and pCO_2 (~650 µatm) for 6 d until hatching.

2.2. pCO_2 treatments

Three pCO_2 treatments were applied, consisting of ambient (~650 µatm, $pH_{Total\ scale}$ 7.82), intermediate (~1500 µatm, pH_T 7.48), and high pCO_2 (~3000 µatm, pH_T 7.18). The ambient pCO_2 treatment served as the control treatment and matched the ambient conditions of the seawater intake, which is representative of current surface ocean conditions in the Salish Sea during spring and summer (Fassbender et al. 2018). The intermediate treatment exceeded the maximum pCO_2 concentrations that seasonally occur in productive nearshore habitats currently but are expected to become increasingly common by the end of this century, and the high pCO_2 treatment is an extreme level that likely exceeded the worst-case scenario for near-future coastal acidification in the Salish Sea (Pacella et al. 2018, Evans et al. 2019).

2.3. Experimental system

Larval Pacific herring were reared through metamorphosis in triplicate 720 l tanks per pCO_2 treatment. Each tank was supplied with single-pass treated seawater (3 l min^{-1}). A natural light cycle ranging from 13 h light:11 h dark to 15 h light:9 h dark was maintained throughout the experiment. Salinity was measured daily (YSI Pro 30) and fluctuated between 28 and 30‰ during the experiment. Tanks were continuously bubbled with laboratory air, ensuring oxygen conditions remained near saturation. Experimental pH and temperature conditions were monitored continuously via an Apex Aquarium Computer System (Neptune Systems). Each replicate tank was outfitted with an Apex PM1 expansion module that controlled laboratory-grade pH and temperature probes positioned near the seawater outlet. Temperatures fluctuated with the ambient seasonal conditions at the laboratory's seawater intake, ranging from 8.8°−12.3°C during the 14 wk rearing period (mean ± SD: 10.5 ± 0.8°C; Fig. S1 in the Supplement at www.int-res.com/articles/suppl/m738p225_supp.pdf). Elevated pCO_2 conditions were controlled via a pH feedback system. When required, the Apex system energized a solenoid valve that directed pressurized CO_2 gas (99% industrial grade; Praxair) through an air diffuser that bubbled directly into each rearing tank. Thorough mixing generated by the flowthrough ensured an even CO_2 dissolution throughout the tank, which was confirmed using a Durafett pH electrode (Honeywell) controlled by a UDA2182 Multiple Input Analyzer (Honeywell International). The CO_2 dosing pressure was carefully calibrated to minimize pH fluctuations. The Durafett electrode was used to verify pH levels via daily spot checks (Fig. S1). All pH probes were cleaned weekly using dilute HCl solution and then recalibrated using 2-point NIST buffers (Thermo Scientific Orion).

2.4. Animal care

On the day of mass hatching (6 d post embryo collection), newly hatched larvae were wet-brailed into each replicate rearing tank (n ≈ 1000 larvae per tank at initiation). Intermediate and high pCO_2 treatments were slowly increased from ambient conditions over 12 and 24 h, respectively. Tanks were greened daily with microalgae concentrate (Nanno 3600, Reed Mariculture). Larvae were fed daily in the morning and weaned to progressively larger food items throughout development. Rotifers *Brachionus plicatilis* were fed-out at an initial tank concentration of 2 prey ml^{-1} from 2 d post-hatch (DPH) to 21 DPH. Enriched (Easy DHA Selco, INVE Thailand) instar-2 *Artemia* nauplii *Artemia franciscana* were introduced at 10 DPH at a rate of 1 prey ml^{-1} and increased to 2 prey ml^{-1} at 22 DPH. Commercially available crumbled fish pellet (Otohime size B2/C2 blend, Marubeni Nisshin Feed Company) was introduced at 63 DPH at ad libitum rations and fed continuously during the day via a belt feeder. As larvae adapted to the pellets, the *Artemia* ration was decreased to 1 prey ml^{-1} at 70 DPH. Tanks were inspected daily for cleanliness, and uneaten food and waste were removed via siphoning. Natural mortalities were not monitored daily, but few (<25 per replicate) accidental deaths associated with cleaning or sampling were observed.

2.5. Carbon chemistry validation

Seawater samples were collected weekly from each replicate tank (n = 15 per replicate) for direct measurements of pH_T and dissolved inorganic carbon (DIC; μmol kg^{-1}). Seawater was filtered (0.2 μm), stored in 60 ml borosilicate BOD bottles, and sealed with glass stoppers lubricated with vacuum grease (Apezion L-type) with no headspace. Samples were stored on ice and processed the following day at the Shannon Point Marine Center Seawater Chemistry Laboratory (Anacortes, WA). Protocols for DIC and spectrophotometric pH measurements closely followed methods described by Love et al. (2017). Samples were warmed to room temperature (22° − 25°C) and then immediately measured for DIC using an Apollo SciTech AS-C3 analyzer that was calibrated with Dickson certified reference materials (batch no. 179; Dickson 2024). Measurements of pH_T were made simultaneously using a diode array spectrophotometer (Agilent 8453A UV-VIS). *In vitro* seawater parameters of pCO_2, total alkalinity (A_T; μmol kg^{-1}), bicarbonate (μmol kg^{-1}), and carbonate (μmol kg^{-1}) were estimated using the R package 'seacarb' (Gattuso et al. 2020) based on direct measurements of DIC and pH_T, the rearing tank salinity and temperature at the time of sampling, and typical nutrient levels for the seawater source (total P: 2.2 μmol kg^{-1}; total Si: 2 μmol kg^{-1}). Constants for K1 and K2 followed Dickson & Millero (1987). The constant for $KHSO_4$ followed Dickson (1990). This method was able to accurately (within ±0.01%) reproduce the A_T of Dickson certified reference materials that were analyzed in parallel with each batch of seawater samples. A summary of carbon chemistry measurements is presented in Table 1.

2.6. Data collection and statistical analysis

All statistical analyses were performed using R (v.4.0.2) in RStudio (v.1.3). Model performance and adherence to assumptions were checked using the R package 'performance' (Lüdecke et al. 2020). Any actions taken to adhere to model assumptions are described below. Statistical significance was determined at $\alpha = 0.05$. The R package 'emmeans' was used for post hoc testing using Tukey's HSD method

Table 1. Replicate mean (±SD) pH_{Total}, pCO_2 (μatm), total alkalinity (A_T; μmol kg^{-1}), dissolved inorganic carbon (DIC; μmol kg^{-1}), bicarbonate (HCO_3^-; μmol kg^{-1}), and carbonate (CO_3^{2-}; μmol kg^{-1}) measured from weekly seawater samples (n = 15)

Tank	Treatment	pH_T	pCO_2	A_T	DIC	HCO_3^-	CO_3^{2-}
1	Intermediate	7.48 ± 0.05	1515 ± 188	2059 ± 23	2076 ± 23	1975 ± 22	33 ± 4
2	Intermediate	7.46 ± 0.04	1570 ± 148	2066 ± 18	2085 ± 23	1983 ± 20	32 ± 3
3	Intermediate	7.48 ± 0.02	1497 ± 77	2064 ± 19	2078 ± 21	1980 ± 19	33 ± 2
4	High	7.17 ± 0.04	3108 ± 294	2052 ± 26	2164 ± 22	2011 ± 24	17 ± 2
5	High	7.20 ± 0.04	2951 ± 251	2052 ± 34	2155 ± 31	2008 ± 32	17 ± 2
6	High	7.19 ± 0.03	2956 ± 202	2051 ± 20	2155 ± 26	2008 ± 22	17 ± 1
7	Ambient	7.82 ± 0.03	662 ± 46	2068 ± 21	1993 ± 22	1894 ± 22	69 ± 4
8	Ambient	7.82 ± 0.03	654 ± 51	2062 ± 24	1986 ± 21	1888 ± 21	70 ± 5
9	Ambient	7.84 ± 0.04	627 ± 67	2068 ± 24	1987 ± 21	1886 ± 21	73 ± 5

where necessary (Lenth 2018). Results are presented as replicate means ± SD unless otherwise noted.

2.6.1. Growth and development

Larval growth and development were compared across the pCO_2 treatments by subsampling herring (n = 5–10 per replicate tank) periodically from 1–98 DPH, totaling 19 sampling events and ~150 fish subsampled per replicate tank. Fish were haphazardly collected with a large aquarium net and immediately euthanized with an overdose of MS-222 (>250 mg l^{-1} seawater solution buffered with bicarbonate to a pH > 7.5). Early larvae were sampled 6 h after feeding live prey items and carefully handled to ensure that stomach contents were not expelled during collection. The offspring were fixed in 10% neutral-buffered formalin for 24 h (48–72 h for larger juveniles) and then transferred to 70% ethanol for storage. Calibrated digital images were made of small larvae (up to 16 DPH) using a digital camera (MC170 HD, Leica Camera) mounted on a dissection microscope (SZ40 stereomicroscope, Olympus) or with a mounted DLSR camera (Nikon 3500, Nikon) and zoom lens for larger larvae (up to 45 DPH). Measurements of standard length (SL; nearest 0.01 mm) and yolk sac area (YSA; 0.01 mm^2) were extracted from images using ImageJ2 (v.2.35; Rueden et al. 2017). Larvae sampled on 3, 5, 8, 13, and 16 DPH were checked for the presence or absence of prey items in the digestive tract. Older larvae and juvenile fish were measured for SL (0.1 mm) with digital calipers. All samples were then dried at 55°C for 24–120 h depending on size and then weighed for dry mass (DM; 0.01 mg) using a micro balance (AT21 Mass Comparator, Mettler Toledo). At 98 DPH, fish were moved to a separate facility for pathogen exposure (see below) or sampled for final growth metrics. Fish in some tanks were maintained for one additional week to facilitate measurements of maximum swim speed.

Pre-flexion stages (1–16 DPH) were analyzed separately because bioenergetic effects associated with elevated pCO_2 are reported most frequently during early larval development (Baumann 2019). Three traits were analyzed for this phase: yolk depletion status (presence or absence of yolk sac), feeding activity status (presence or absence of rotifers in gut), and growth (SL and DM). Logistic regression was used to test for pCO_2 × age effects on the binary traits of yolk depletion and feeding activity using generalized linear mixed effects models (GLMMs) that assumed a binomial distribution (link function = logit) using the R package 'lme4' (Bates et al. 2015) with p-values calculated by the 'lmerTest' package (Kuznetsova et al. 2017). The model included pCO_2 treatment as a fixed factor, age as a continuous covariate, and their interaction. To account for the fact that multiple fish were sampled from the same replicate tank at each time point, a random coefficient term was included that allowed the model to consider variation of intercepts and slopes among different replicates. The model formulation in R was:

$$\text{Yolk depletion status (or feeding activity status)} \sim \text{age} \times pCO_2 + (1 + \text{age} \mid \text{tank})$$

Effects of pCO_2 on early larval growth (SL and log-transformed DM) were tested via linear mixed-effects models (LMMs) that assumed a Gaussian distribution. Measurements from individual larvae were tested using pCO_2 treatment as a fixed factor, age as a continuous covariate, their interaction, and replicate tank was included as a random intercept and slope coefficient term:

$$\text{SL (or Log[DM])} \sim \text{age} \times pCO_2 + (1 + \text{age} \mid \text{tank})$$

Additional LMMs were constructed to test for long-term pCO_2 × age effects on SL and log-transformed DM over the entire rearing interval (1–98 DPH) and were analyzed using the same model format as described for larval growth. To test whether pCO_2 treatment influenced the length-to-weight relationship of developing herring (as an indicator of body condition), replicate mean values for SL and DM were calculated for each sampling timepoint between 1 and 98 DPH. The effect of treatment pCO_2 was tested using a generalized additive model to fit the non-linear relationship between log-transformed DM and log-transformed SL using the R package 'mgcv' (Wood & Wood 2015). The final model formulation in R was:

$$\text{log(mean\_DM)} \sim \text{s(log(mean\_SL), bs = 'tp', k = 5)} + pCO_2$$

An overall survival ratio was calculated for each replicate tank as the number of juveniles surviving to 98 DPH minus the sum of subsampled fish plus incidental mortalities all divided by 1000 starting larvae. ANOVA was used to test for a pCO_2 effect on logit-transformed survival ratio (Warton & Hui 2011).

2.6.2. Maximum swim speed

Swimming performance of juvenile herring (90–105 DPH; 50–68 mm SL) in each pCO_2 treatment (n = 5 fish $tank^{-1}$; 45 fish total) was evaluated using a con-

stant acceleration test to evaluate maximum swim speed (U_{max}; Farrell 2008). We used a modified Blazka-type swim tunnel with a 1.5 l swim chamber (Loligo Systems) outfitted with a SEW Eurodrive motor and power inverter for fine-scale control over flume speed. The swim chamber was enclosed within 2 honeycomb baffles to promote a lamellar flow. Flow speed through the chamber was calibrated to power supply voltage output by recording the passage of dilute green dye injected into the chamber as it transited across a scale-bar using a high-speed video camera (60 frames s^{-1}, GoPro Hero10) at 9 different voltages across the range of motor outputs (73 captures total). Flow speed was determined in ImageJ2 by measuring the distance traveled by the leading edge of the dye during the image capture. A linear regression fitting dye speed to voltage output ($R^2 = 0.977$) was used to estimate flume speed at all voltage outputs.

Individual fish were transferred from rearing tanks to the swim chamber on the day of testing (prior to feeding) using a bucket to minimize collection stress and injury, and then carefully poured into the swim chamber through a funnel. The chamber received a continuous supply of oxygenated seawater that was adjusted to the current temperature and pCO_2 conditions of the respective rearing treatment. Temperatures ranged between 12° and 13.5°C across trials. Fish were acclimated to a swim speed of 15 cm s^{-1} for 20 min. Providing the fish with a moderate starting swim speed had the effect of greatly reducing visible signs of stress associated with confinement, but a small number (<10 total) of distressed individuals that showed erratic swimming behavior were removed and replaced. After acclimation, flow speed was incrementally increased by 1 cm s^{-1} every 1 min until the fish was unable to swim for a complete minute at a given speed (Farrell 2008). Failure was assigned when the fish remained in continuous contact with the back screen for 15 s. The failure timer was reset if the fish resumed swimming before 15 s and was able to remain off the back screen for 5 s. Post-trial, each fish was euthanized, measured for SL and wet mass (WM), preserved in 10% neutral buffered formalin for 24 h, and then transferred to 70% ethanol for additional measurements to be reported elsewhere. U_{max} was calculated as $U_{max} = U + (t \times t_i^{-1} \times U_i)$, where U (cm s^{-1}) is the final speed attained by the fish, t (s) is the time spent swimming at final speed, t_i is the time interval per velocity increment (60 s), and U_i is the velocity increment (1 cm s^{-1}) (Brett 1964).

A condition factor (k) was computed for each swimmer as $k = 100 \times WM_{(g)} / SL^3_{(cm)}$. The SL, WM, and k of swimmers tested are shown in Fig. S2; morphometric traits did not vary significantly by pCO_2 treatment (Fig. S2). The effect of pCO_2 treatment on U_{max} was tested using a mixed-effect ANOVA (Satterthwaite's degrees of freedom method) using the 'lme4' and 'lmerTest' R packages. pCO_2 treatment was set as a fixed factor and linear covariates were added that could affect swimming performance, including SL, k, age of the fish (days), mean water temperature during the trial, and the hour of day that the trial was completed. A random intercept term for replicate tank was added to account for fish sampled from the same rearing tank:

$$U_{max} \sim pCO_2 + SL + k + age + temperature + hour + (1 \mid tank)$$

2.6.3. Pathogen challenge

We applied well-established protocols for VHS challenge experiments focused on juvenile Pacific herring (Hershberger et al. 2013, 2021a). The influence of pCO_2 on VHS susceptibility was assessed by exposing groups of age 0 yr juvenile herring (98 DPH; 48.5 ± 4.5 mm SL) from each of the pCO_2 treatments to VHSV. To facilitate viral exposures, a separate experimental setup was prepared in a quarantine facility, composed of nine 265 l cylindrical tanks (n = 3 tanks per pCO_2 treatment). An identical 9-tank setup was prepared in an adjacent quarantine facility to serve as negative controls (n = 3 tanks per pCO_2 treatment). All tanks were stocked with 60 herring (n = 60 per tank), representing 20 fish that were sampled from each of the original triplicate pCO_2 rearing tanks and pooled together. At initial stocking, tanks were filled with seawater that was adjusted to match the pCO_2 and temperature conditions in the original rearing tanks. However, due to safety regulations that prevent equipment from being moved in and out of the quarantine facilities, the manipulation of seawater pCO_2 was not possible during the pathogen challenge. Consequently, once stocked, all tanks received a continuous supply (3.5 l min^{-1}) of processed (sand-filtered, particle-filtered to 10 µm, and UV-irradiated) seawater and were bubbled with laboratory air so that tanks slowly equilibrated to ambient pCO_2 conditions within 6 h of stocking and prior to the addition of virus. Ambient pCO_2 was maintained in all replicate tanks throughout the challenge. Roughly 42 h after stocking, the flowthrough was discontinued to the tanks, water levels were lowered to 100 l, and aliquots of stock virus (VHSV genotype IVa, isolate #Her 5, originally isolated from Pacific herring in Elliott Bay, Puget Sound, WA in

2002) were added to the experimental tanks; mean waterborne exposure levels were titered at 807 plaque-forming units (PFU) ml^{-1}. Negative control tanks were exposed to phosphate-buffered saline in lieu of virus. After the 2 h exposure period, seawater supply to the tanks was resumed, and water volumes in the flow-through tanks were maintained at 265 l for the remainder of the experiment.

Tanks were checked for dead fish (designated as 'mortalities') every 24 h and fed ad libitum rations of pellet food 3 times per week. The challenge was terminated 28 d post-exposure (DPE), and remaining fish were designated as 'survivors' and were euthanized. All mortalities and euthanized survivors from VHSV-exposed tanks were measured for SL, WM, and k, and were dissected to remove kidney and spleen. We used mixed-effects ANOVAs to test whether SL, WM, and k of mortalities and survivors varied between pCO_2 treatments. Plaque assay on polyethylene glycol-pretreated EPC cells (Batts & Winton 1989) was used to test for the presence of VHSV in kidney and spleen pools. The plaque assay limit of detection was 400 PFU g^{-1}. A ratio of viral prevalence (i.e. VHSV positive or VHSV negative) detected in trial mortalities and final survivors was calculated for each replicate tank. The effect of pCO_2 treatment on the viral prevalence ratio was tested with a one-way ANOVA. Ratio data were logit transformed prior to testing.

A survival analysis was used to estimate the daily likelihood of death (i.e. an event hazard) after VHSV exposure. Given the observed evidence of non-proportional hazards between treatment groups, a weighted Cox regression was preformed using the R package 'coxphw' (Dunkler et al. 2018). This approach enables the estimation of average hazard ratios (±95% confidence intervals) by incorporating Prentice weights for right-censored data (Schemper et al. 2009). A fish's event time (days) and status (i.e. dead or censored) were modeled as a function of virus exposure (negative control or VHSV) and the interaction between virus exposure and pCO_2 treatment. The model formulation in R was:

coxphw(Surv(time, status) ~ virus × virus:pCO_2, template = 'AHR')

The model output provided hazard ratios which estimated the factorial change in the likelihood of VHS-induced mortality with exposure to elevated pCO_2 treatments relative to fish reared under ambient pCO_2. We ran a second model with the intermediate pCO_2 coded as the reference treatment to estimate the change in hazard ratio between intermediate and high pCO_2. For VHSV-treated groups, we conducted additional weighted Cox regressions to examine whether variations in SL and k influenced VHS mortality. To remove the effect of growth during the trial, we computed a residual SL from the linear fit between SL and age at death or censoring for all VHSV-exposed samples (mortalities and survivors) combined across pCO_2 treatments ($R^2 = 0.161$, $p < 0.001$). The Cox regression formulation in R was:

coxphw(Surv(time, status) ~ pCO_2 + residual.SL + k, template = 'AHR').

3. RESULTS

3.1. Early larval development

There was no effect of pCO_2 treatment on the growth rate of pre-flexion larvae as determined by slope coefficients for SL and DM, which were similar between pCO_2 treatments (Fig. 1A,B, Table 2, Table S1). While growth rate did not vary, larvae sampled from the intermediate pCO_2 treatment were smaller during the early larval phase (−3.5% with respect to SL and DM) than samples from the ambient pCO_2 treatment, although the effect was only significant for SL (LMM, $t_{538} = -2.022$, $p = 0.044$) and not DM (Table S1). By 3 DPH, roughly half of all larvae sampled had fully consumed their yolk reserves and yolk depletion rates increased to ~95% by 5 DPH, with no indication of differential effects of pCO_2 on time to yolk depletion (Fig. 1C, Table S1). Feeding activity was variable between replicate tanks at 3 DPH, but increased with age from 44 ± 23% at 3 DPH to 86 ± 16% at 5 DPH and remained >90% on average through 16 DPH (Fig. 1D). The increase in feeding rate was noticeably slower for larvae reared under intermediate pCO_2, but not significantly different from controls (GLMM, $z = -1.435$, $p = 0.151$; Table S1).

3.2. Long-term growth and survival

Long-term growth rate was not significantly affected by pCO_2 treatment with respect to SL and DM (Fig. 2A,B, Table 2, Table S2). Larval growth slowed substantially in one of the high pCO_2 replicates (Tank 5) between 60 and 90 DPH but then showed an indication of growth compensation by the final sample (Fig. 2A,B). There was no effect of pCO_2 treatment on the length-to-weight relationship (Fig. 2C, Table S2). Survival rates for replicate tanks measured

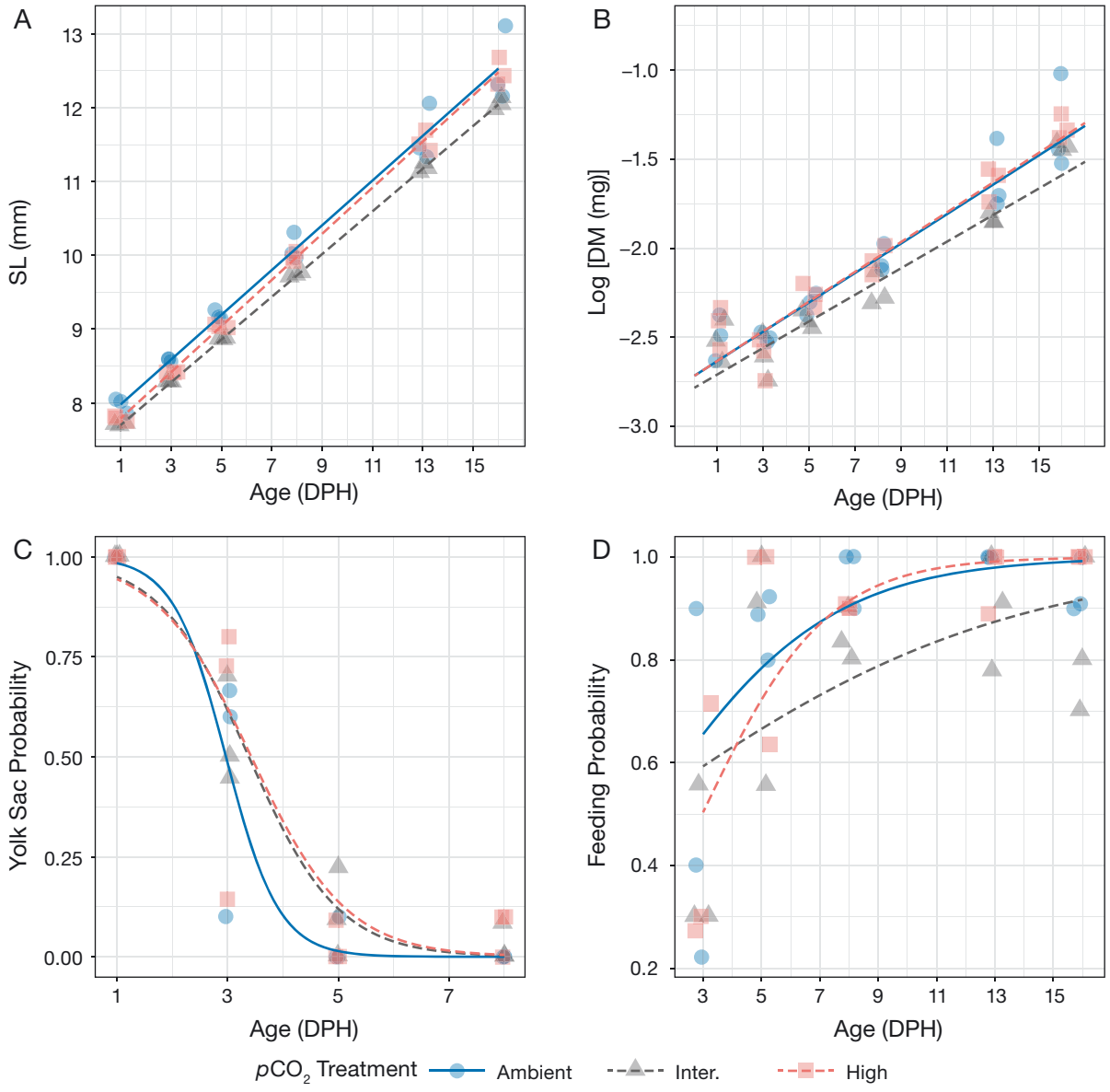

Fig. 1. Linear growth trajectories for (A) standard length (SL) and (B) log-transformed dry mass (DM) of pre-flexion Pacific herring *Culpea pallasii* larvae. Logistic regression fits for the ratio of larvae (C) with remaining yolk reserves and (D) actively feeding. Colored symbols: mean values for each replicate tank; lines: regression fits by pCO_2 treatment. DPH: days post-hatch; Inter.: intermediate treatment

from hatch to 98 DPH ranged from 30–41% (overall mean: 37.7 ± 3.7%) and were not affected by pCO_2 treatment (Table S3).

3.3. Maximum swim speed

U_{max} was not significantly affected by pCO_2 treatment (mixed-effect ANOVA, $F_{2,37} = 2.048$, p = 0.143). Average U_{max} was higher in juveniles from ambient pCO_2 (45.7 ± 16.3 cm s^{-1}) compared to those reared under intermediate (38.6 ± 12.8 cm s^{-1}) and high (36.9 ± 14.3 cm s^{-1}) pCO_2 treatments (Fig. 3). Swimming performance was considerably variable, with individual U_{max} varying by up to 3-fold within treatment groups (Fig. 3). Fish reared under ambient pCO_2 conditions made up the majority (58.3%) of the highest-performing swimmers (i.e. ranked above the 75% percentile) (Fig. 3). None of the tested covariates had a significant influence on U_{max} (Table S3), and the stepwise removal of covariates from the model did not alter the significance level associated with pCO_2 treatment.

Table 2. Growth regressions fitted to standard length (SL) and dry mass (DM) of Pacific herring *Clupea pallasii* offspring during pre-flexion development (1–16 d post-hatch) and across the entire rearing trial (1–95 days post hatch). Standard errors for intercept and slope coefficients are shown in parentheses. The total number of fish included for each regression fit (n) and the adjusted r squared for each regression fit (adj. R^2) are listed

pCO_2 treatment	Trait	Regression	n	Adj. R^2
Pre-flexion larvae				
Ambient	SL	7.67 (±0.09) + 0.30 (±0.01) × age	185	0.82
	DM	0.066 (±0.049) + $e^{0.083(\pm0.008) \times age}$	184	0.69
Intermediate	SL	7.41 (±0.13) + 0.29 (±0.01) × age	181	0.81
	DM	0.062 (±0.070) + $e^{0.075 (\pm0.008) \times age}$	177	0.64
High	SL	7.48 (±0.13) + 0.31 (±0.01) × age	174	0.89
	DM	0.066 (±0.070) + $e^{0.084 (\pm0.008) \times age}$	173	0.74
Full trial				
Ambient	SL	6.78 (±0.29) + 0.38 (±0.016) × age	463	0.95
	DM	0.072 (±0.036) + $e^{0.088 (\pm0.002) \times age}$	463	0.98
Intermediate	SL	6.37 (±0.41) + 0.40 (±0.022) × age	457	0.96
	DM	0.064 (±0.051) + $e^{0.091 (\pm0.003) \times age}$	452	0.97
High	SL	7.18 (±0.41) + 0.36 (±0.022) × age	450	0.95
	DM	0.078 (±0.051) + $e^{0.084(\pm0.003) \times age}$	450	0.98

3.4. VHSV challenge

The survival of uninfected fish from the negative control group was nearly 100% across pCO_2 treatments (Fig. 4A). By contrast, herring from all pCO_2 treatments were highly susceptible to VHS, as the onset of virus-positive mortalities began at 4 or 5 DPE in all replicate tanks (Fig. 4A). Daily mortality rates were highest during the initial phase of the disease outbreak, particularly amongst fish reared under high pCO_2, which showed the highest single-day mortality event at 5 DPE (Fig. 4B). At trial termination (28 DPE), cumulative percent mortality was highest in fish reared under high pCO_2 (54.8 ± 15.2%) compared to intermediate (40.4 ± 4.5%) and ambient pCO_2 groups (46.7 ± 14.8%), respectively (Fig. 4A). Survival analysis indicated that probability of mortality was significantly greater in fish reared under the high pCO_2 treatment relative to groups from ambient pCO_2 (hazard ratio = 1.34, p = 0.046; Table 3) and intermediate pCO_2 (hazard ratio = 1.60, p = 0.002, Table 3). Hazard ratios were not significantly different between the ambient and intermediate pCO_2 treatments (Table 3). VHSV was detected in the kidney and spleen of 87% of mortalities collected during the trial and viral prevalence was similar across treatments (Fig. 5A, Table S4). Only 1.4% of fish that survived to 28 DPE showed positive viral titers (Fig. 5B), with no effect of pCO_2 (Table S4).

Across pCO_2 treatments, survivors were longer (+4.7 mm) and heavier (+0.34 g) than mortalities, indicating that surviving fish continued to grow during the trial (Fig. 5C–F). Mortalities and survivors from the intermediate pCO_2 treatment were significantly longer and heavier than fish from the high pCO_2 treatment (Tukey's HSD, $p < 0.05$), while the size of fish from the ambient pCO_2 treatment was similar to both intermediate and high pCO_2 treatments (Fig. 5C–F, Table S5). Survival analysis revealed that residual SL did not influence the risk of mortality (hazard ratio = 1.00, p = 0.873; Table S6), indicating that increased VHS mortality under high pCO_2 was not attributable to a smaller average size. The *k* of mortalities was similar across pCO_2 treatments, whereas the *k* of survivors from the high pCO_2 treatment was significantly lower (−18.2%) relative to survivors from the ambient and intermediate pCO_2 treatments (Tukey's HSD, $p < 0.01$; Fig. 5, Table S5). Condition factor did not significantly influence the risk of mortality in VHSV-treated groups (hazard ratio = 2.18, p = 0.086; Table S6).

4. DISCUSSION

4.1. CO_2 effects on pathogen susceptibility

Ocean acidification has the potential to alter organismal resistance to infectious diseases, yet very few studies have evaluated those impacts on marine fish (Burge & Hershberger 2020, Cohen-Rengifo et al. 2022). For the first time, we tested how chronic exposure to elevated pCO_2 affects the susceptibility of Pacific herring to the endemic viral pathogen VHSV. Treatment groups of herring that were reared for 14 wk under intermediate pCO_2 (1500 µatm) showed similar disease susceptibility as those from the ambient pCO_2 treatment (650 µatm), with no indication of differential effects on the timing and probability of host infection and mortality. By contrast, herring reared under a more extreme pCO_2 treatment of 3000 µatm showed modest differences in the progression of disease. The acute mortality phase peaked earlier relative to the other treatments, and VHS-related mortality was significantly higher than in herring reared under the ambient and intermediate pCO_2

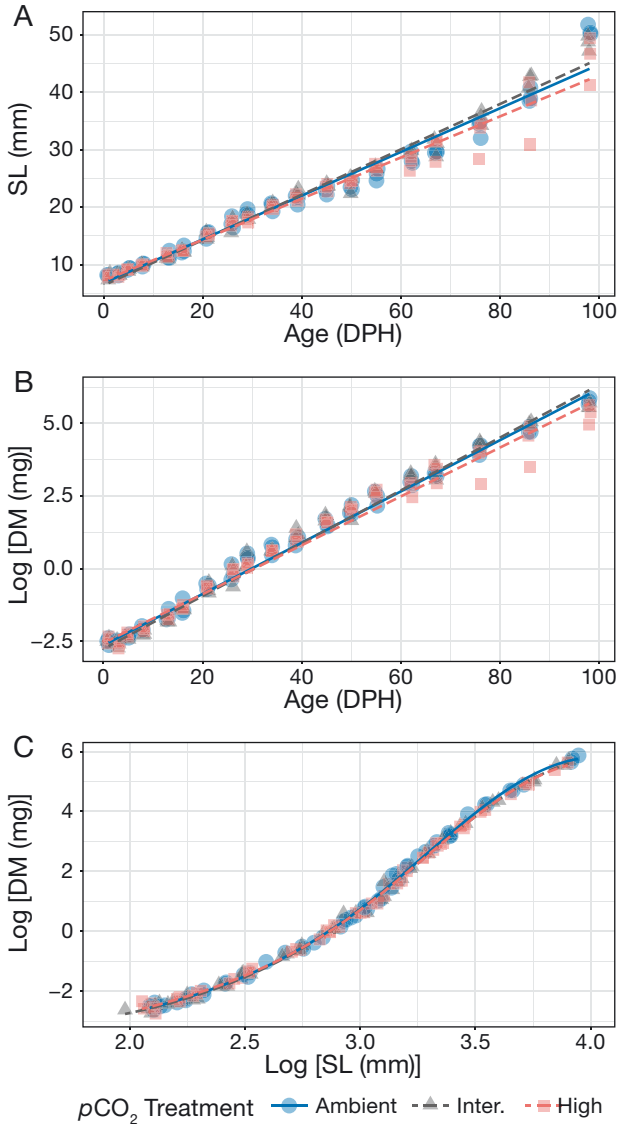

Fig. 2. Long-term growth trajectories for (A) standard length (SL) and (B) log-transformed dry mass (DM) of Pacific herring *Culpea pallasii* reared under 3 pCO_2 treatments from 1–98 d post-hatch (DPH). (C) Log-transformed SL to DM relationship by pCO_2 treatment for the entire rearing interval. Colored symbols show replicate mean values for each sampling point while lines denote linear regression (SL and DM) or generalized additive model fits (SL to DM relationship) by pCO_2 treatment

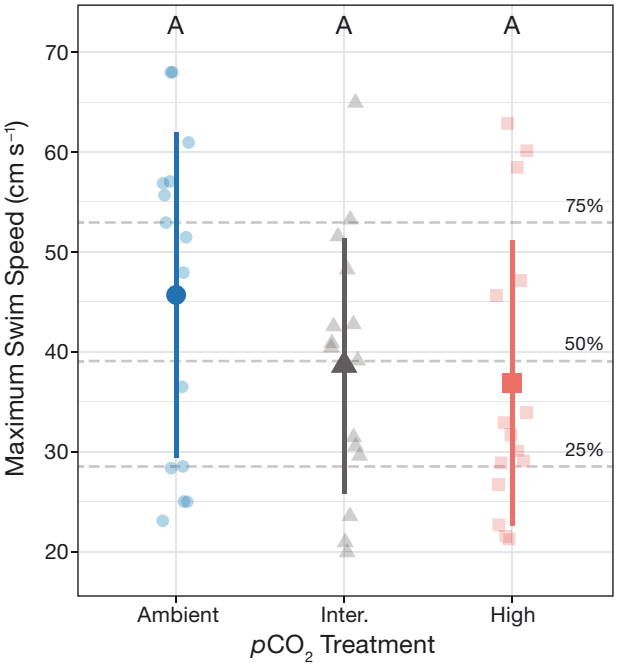

Fig. 3. Maximum swim speed (U_{max}) of juvenile Pacific herring *Clupea pallasii* reared under 3 pCO_2 treatments. Large colored symbols: treatment means; vertical lines: ±SD; small faded symbols: U_{max} for individual fish; horizontal dashed lines: quartiles calculated from U_{max} values pooled across pCO_2 treatments. Similar letters above bars indicate non-significant differences between treatment groups (Tukey's HSD)

treatments. This suggests that chronic exposure to extreme high pCO_2 conditions depressed the antiviral immune response in the exposed herring, leading to increased rates of initial infection, transmission, and mortality. The prevalence of the infection in trial mortalities, as indicated by positive VHSV titers in kidney–spleen homogenates, was high and roughly the same across treatment groups. Furthermore, nearly all fish that survived to the end of the trial were negative for VHSV regardless of treatment. However, survivors from the high pCO_2 treatment exhibited poorer body condition than survivors from the ambient and intermediate pCO_2 treatments. This suggests that the immune response of high pCO_2 juveniles may have led to heightened metabolic dysfunction, potentially due to an inefficient response, increased energetic costs, or reduced appetite (although no discernible differences in feeding behavior were observed).

These findings carry implications for VHS epizootiology within coastal ecosystems of the North Pacific, where ocean acidification is progressing faster than the global average (Cai et al. 2021) and where Pacific herring are a major reservoir species for the virus (Hershberger et al. 2016). While specific projections remain uncertain, it is possible that by the year 2100, maximum daily pCO_2 in the Salish Sea and nearby coastal ecosystems may reach about 1500 µatm, and this condition may persist for weeks or months at a time (Pacella et al. 2018, Evans et al. 2019). Importantly, our results demonstrate that chronic exposure to this level of acidification is unlikely to increase herring susceptibility to VHS. However, the negative

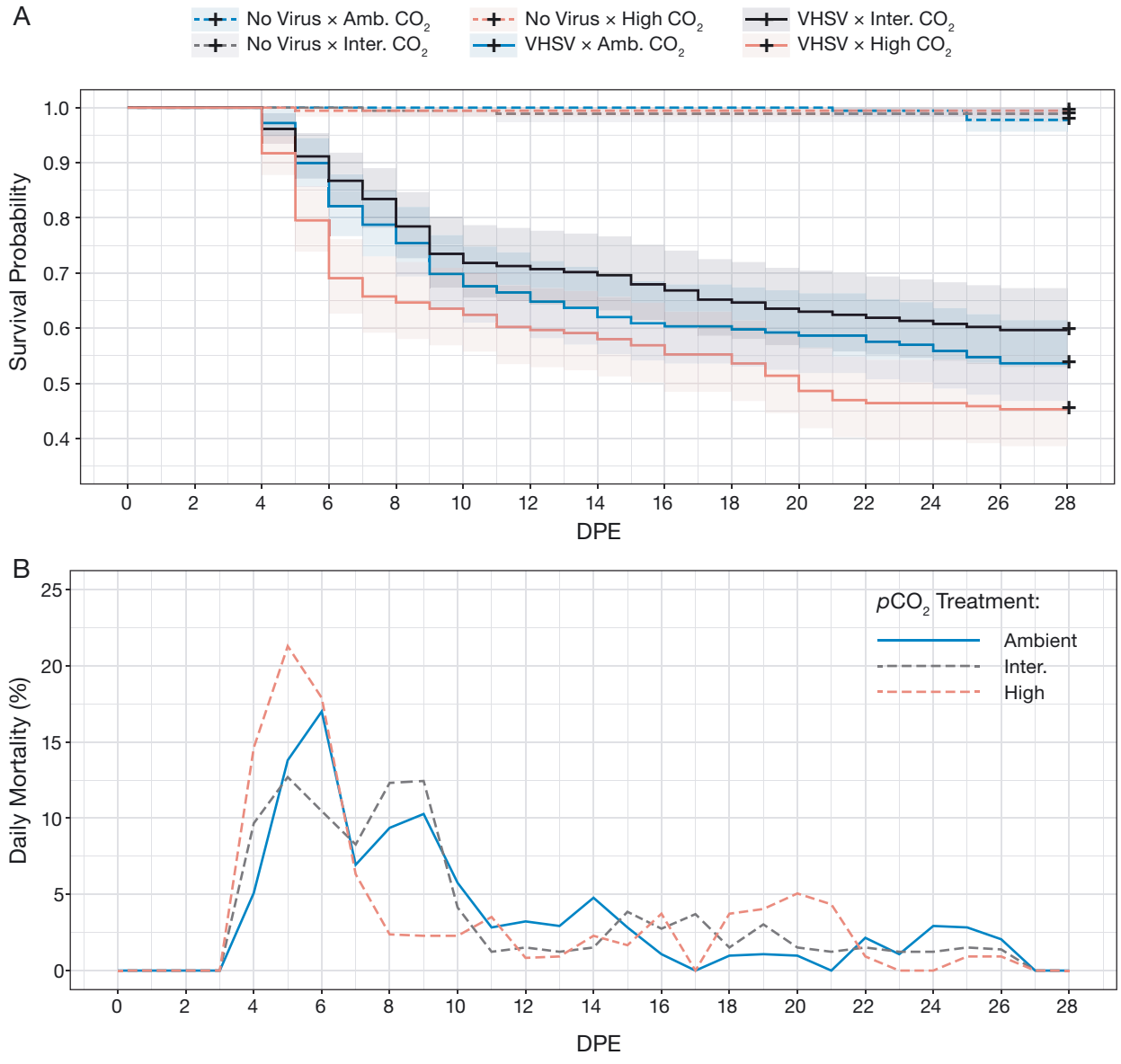

Fig. 4. (A) Kaplan-Meier plot of the survival probability of Pacific herring *Culpea pallasii* as a function of time (days post exposure, DPE) for juveniles exposed to VHSV (viral hemorrhagic septicemia virus; solid lines) or buffer only (no virus, dotted lines) crossed with 3 pCO_2 rearing treatments. Shaded areas: ±95% confidence intervals of survival probabilities. (B) Percent average daily mortality (daily mortality divided by final cumulative mortality) of juveniles after water-borne exposure to VHSV

effects observed in fish reared under 3000 µatm pCO_2 suggest that prolonged exposure to extreme pCO_2 conditions can impair immunological responses. Such a high level of pCO_2 is expected to remain infrequent in coastal habitats of the Northeast Pacific, even under the most severe CO_2 emission scenarios, and may only manifest during brief periods of intense net community respiration (Pacella et al. 2018). Even so, any factors that enhance disease amplification will promote the formation of VHS outbreaks in wild populations (Hershberger et al. 2016). Thus, additional evidence targeting specific immune markers is needed to better understand potential immunological effects associated with exposure to extreme acidification, particularly under fluctuating regimes that mimic natural and future pCO_2 variability in productive coastal habitats.

In contrast to our results, a recent study demonstrated a clear immunoenhancing effect in European seabass reared under 1700 µatm pCO_2, as mortality resulting from exposure to a betanodavirus was reduced by 79% (Cohen-Rengifo et al. 2022). Increased

Table 3. Cox regression analysis assessing the impact of viral hemorrhagic septicemia virus (VHSV) exposure and pCO_2 rearing treatment on the survival of juvenile Pacific herring *Clupea pallasii*. Two models are presented with ambient and intermediate pCO_2 as reference treatments to test all treatment comparisons. Model outputs include the hazard ratio (HR) associated with VHSV exposure for the reference pCO_2 treatment and the factorial change to HR for the other pCO_2 treatments relative to the reference treatment. HRs are presented as 95% confidence intervals (CIs) and effects that reached statistical significance are indicated by **bold** p-values

Factor	HR	HR 95% CI	*z*	p
Ambient pCO_2 as reference treatment				
Ambient pCO_2	48.68	22.58–104.97	9.911	**<0.001**
Ambient vs. intermediate pCO_2	0.84	0.63–1.13	−1.157	0.247
Ambient vs. high pCO_2	1.34	1.00–1.78	1.991	**0.046**
Intermediate pCO_2 as reference treatment				
Intermediate pCO_2	40.68	18.78–88.10	9.397	**<0.001**
Intermediate vs ambient pCO_2	1.20	0.88–1.62	1.157	0.247
Intermediate vs. high pCO_2	1.60	1.19–2.15	3.099	**0.002**

survival corresponded with an upregulation of innate antiviral immune factors within the olfactory rosette of exposed fish, including enriched gene sets involved in pathogen recognition and interferon signaling (Cohen-Rengifo et al. 2022). Similar transcriptional patterns have been observed in several other species of marine fish, suggesting that increased innate immune function may be a common by-product of acclimation to elevated pCO_2 (Bresolin de Souza et al. 2016, Huth & Place 2016, Toy et al. 2022). The early anti-viral innate immune response becomes elevated during the early days after VHSV exposure in Pacific herring and can provide some protection if upregulated early enough (Hansen et al. 2012). However, our study did not provide phenotypic evidence that this transcriptional response was further enhanced by exposure to elevated pCO_2 conditions, as herring in the intermediate treatment (1500 µatm pCO_2) showed similar susceptibility to VHS as conspecifics reared under ambient pCO_2 conditions. Interspecific variation is a prominent feature of biological responses to ocean acidification, and differences in experimental methodologies can add to this variation (Baumann 2019). For example, the European seabass investigated by Cohen-Rengifo and colleagues were the F2 progeny of a long-term, multigenerational experiment (Mazurais et al. 2021), and thus the processes of intergenerational acclimation may have canalized transcriptional pathways associated with enhanced antiviral immunity in the F2 generation (Munday 2014).

However, divergent responses to elevated pCO_2 also reflect evolutionary differences among species, shaped by the natural pCO_2 variability experienced by a species during its evolutionary history (Kang et al. 2022). It may be that organisms inhabiting naturally acidified marine ecosystems, like Pacific herring in the Salish Sea, are adapted to elevated pCO_2 and less susceptible to changes in immune function (Baumann 2019). Furthermore, experimental constraints prevented the continuation of pCO_2 treatments during the pathogen challenge, and herring reared under elevated pCO_2 were gradually conditioned to ambient pCO_2 2 d before viral exposure. This transition likely affects the same biochemical processes as an initial exposure to acidified conditions (Brauner et al. 2019) and fluctuating pCO_2 can elicit different molecular responses compared to static exposures, including for genes involved in regulating immunity (Schunter et al. 2021). Thus, shifting juveniles from elevated to ambient pCO_2 may have influenced how these groups responded to VHS, or even been the main factor responsible for it. Consequently, the limited available evidence constrains our ability to make broader predictions of how ocean acidification will influence host–pathogen interactions in fish. Further research is needed to resolve these uncertainties, especially studies that consider life stage, exposure duration, and potential interactions with fluctuating and multistressor environments.

For example, temperature is a major environmental factor controlling the development of VHS epizootics in Pacific herring. Warm conditions promote the rapid upregulation of a type I interferon response, which provides a robust first line of defense against VHSV infection and greatly suppresses viral transmission (Hershberger et al. 2013). It should be noted that the present study coincided with a historic heatwave in the Pacific Northwest (June–July 2021; Philip et al. 2021). Consequently, the ambient seawater in our experimental facility was unseasonably warm during the disease challenge, averaging 12.9°C compared to typical July temperatures of around ~10.5°C. These warm conditions resulted in the modest levels of observed overall VHS mortality (~47%). By contrast, experiments conducted at 9°C have produced mortality rates in excess of 80%, using the same viral exposure methods applied here (Hershberger et al. 2013). While we can only speculate, it is possible that the warm, immune-enhancing conditions may have masked secondary immune effects (positive or negative) associated with pCO_2 exposure history. Given that spawning in most Pacific herring stocks in the

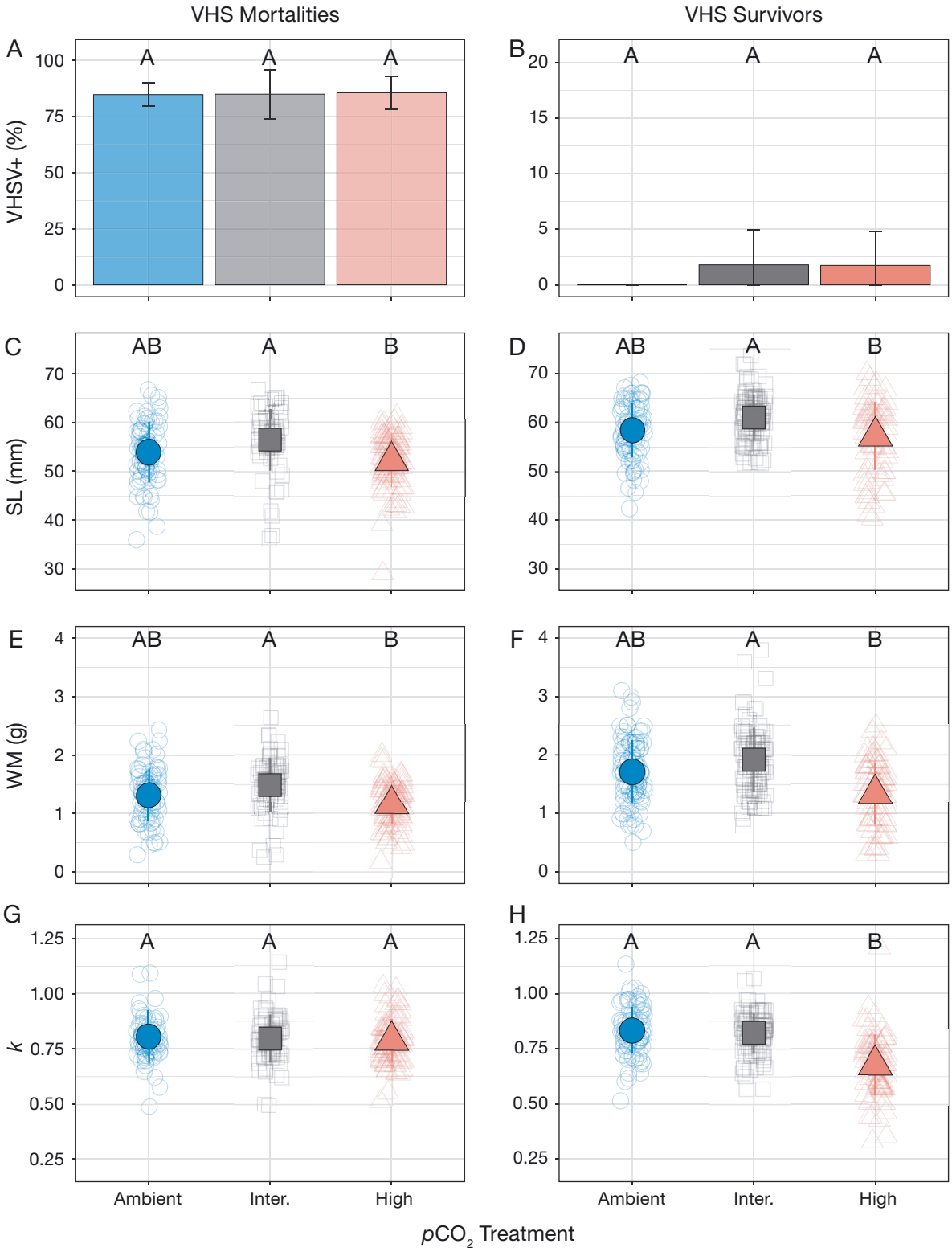

Fig. 5. Mean (±SD) percentage of viral hemorrhagic septicemia virus (VHSV)-positive (A) mortalities and (B) survivors of Pacific herring *Culpea pallasii* collected during the disease challenge. The (C,D) standard length (SL), (E,F) wet mass (WM), and (G,H) condition factor (*k*) of viral hemorrhagic septicemia (VHS) mortalities and survivors. Large solid symbols: pCO_2 treatment means; vertical lines: ±SD; faded shapes: individual fish. Results of pairwise comparison post hoc tests are shown as letters above bars, where differing letters indicate significant differences between treatment groups (Tukey's HSD, $p < 0.05$)

Salish Sea occurs during late February and early March (Sandell et al. 2019), it is important to explore the effects of elevated pCO_2 on immune responses to VHS under cooler conditions that newly metamorphosed juveniles typically encounter (Hershberger et al. 2013).

4.2. CO_2 effects on early larval development

We focused on assessing potential CO_2 effects on pre-flexion larvae, which may exhibit a heightened sensitivity to future pCO_2 because they lack developed gills with Na^+/K^+-ATPase-rich ionocytes, which effectively maintain blood acid–base balance in older fish (Perry & Gilmour 2006, Ishimatsu et al. 2008). Furthermore, early development operates on a tight metabolic budget as larvae balance the energy required to fuel rapid growth and the increasing demands associated with swimming and foraging during the transition from endogenous to exogenous feeding (Rombough 2006). We hypothesized that acidified conditions would result in a metabolic tradeoff, as larvae divert energetic resources towards critical homeostatic mechanisms at the expense of growth. However, in contrast to expectations, rates of growth and endogenous energy use of pre-flexion larvae were very similar across pCO_2 treatments. Larvae reared under ~1500 µatm pCO_2 were slightly smaller during this interval, which coincided with a non-significant reduction in feeding activity. Neurological disturbances are a common response to elevated pCO_2 and disruptions to sensory recognition systems could affect the ability of fish larvae to detect and capture prey (Heuer et al. 2019). However, larvae reared under ~3000 µatm pCO_2 showed no effect on feeding rates or size, and the growth effect observed under intermediate pCO_2 did not extend beyond the pre-flexion stage. These findings, combined with previous studies focused on the embryonic stage of Pacific herring (Frommel et al. 2022, Murray & Klinger 2022, Singh et al. 2023) demonstrate that the early life stages of this species can tolerate elevated pCO_2 consistent with future levels of ocean acidification predicted for the region, likely through the rapid proliferation of robust acid–base regulatory systems early in development (Dahlke et al. 2020, Kwan et al. 2021). Our results add to the growing body of research showing that species such as Pacific herring that reproduce in highly variable environments prone to large pCO_2 fluctuations produce offspring with a high tolerance to acidified conditions (Murray et al. 2014, Baumann 2019).

4.3. Chronic effects of elevated pCO_2 on growth and U_{max}

While most fish exhibit robust capacities to buffer against short-term exposures to acidification, the prolonged maintenance of such altered biochemical states could have a metabolic cost over longer-term exposures spanning multiple life stages (Murray et al. 2017). However, in this study, we found that chronic exposure to either 1500 or 3000 µatm pCO_2 did not significantly affect the growth or body condition of larvae and juveniles during the initial 14 wk of development. This suggests that Pacific herring may experience minimal energetic costs from the molecular response to acidification over the long term, or that any incurred costs can be offset without metabolic tradeoffs. This finding is consistent with studies focused on Atlantic herring (Stiasny et al. 2016, Sswat et al. 2018, Joly et al. 2023) and other temperate and tropical fish species (Hurst et al. 2012, Jarrold & Munday 2018, Sundin et al. 2019) that have shown robust long-term growth responses to elevated pCO_2.

However, this response was not universal across all rearing tanks, as herring from a single high pCO_2 replicate exhibited a pronounced decline in growth rate, beginning ~25–30 mm SL (or 60 DPH). This size range marks the onset of metamorphosis in Pacific herring (Stevenson 1962), and energetic stress is a primary cause of delayed metamorphosis in fish (Pechenik 2006). A similar response has been documented in Atlantic herring larvae reared under ~1800 and ~4200 µatm pCO_2 (Frommel et al. 2012), suggesting that shifts in energy management could underlie the observed growth responses to elevated pCO_2 in certain species (Ruiz-Jarabo et al. 2021). Water quality and ration levels were carefully monitored throughout the rearing trial, and we do not believe this outlying growth response was caused by uncontrolled factors. Yet the lack of observable responses in other replicates prevents us from definitively linking the effect to high pCO_2 exposure. More research is needed to understand the impacts of extreme acidification on the intermediary metabolism of developing herring, particularly during metamorphosis.

Swimming performance is a key determinant of individual fitness and could be affected by elevated pCO_2 through impacts on oxygen acquisition and delivery, increased risk of respiratory acidosis, changes to morphology, and energy limitation (Kunz et al. 2018, Vilmar & Di Santo 2022). However, the available experimental evidence suggests that the swimming traits of most larval and juvenile fish are not affected by elevated pCO_2 (Cominassi et al. 2019,

Downie et al. 2020). Even so, significant reductions to maximum aerobic and anaerobic swimming capacity have been observed in Polar cod *Boreogadus saida* exposed to 1170 µatm pCO_2 for 4 mo, suggesting that long-term exposures could cause negative effects (Kunz et al. 2018). Our results align with broader findings in that exposure to elevated pCO_2 during larval development did not significantly alter the U_{max} of juvenile Pacific herring. However, this result is associated with some uncertainty. Juveniles reared under 1500 and 3000 µatm pCO_2 treatments showed an average reduction in U_{max} by 15.5 and 19.5%, respectively, compared to fish from ambient pCO_2. Yet substantial intra-treatment variability rendered the effect nonsignificant, as multiple fish in each treatment failed to maintain position in the flume at relatively low speeds. In some cases, premature failure likely occurred due to a behavioral response to isolation, confinement, and forced swimming rather than metabolic fatigue (Peake & Farrell 2006). It is worth noting that a recent study that tested groups of Pacific herring in a larger swim flume produced similar variability (Sewall et al. 2021). Alternative methods to forced swimming within a narrow flume may be better suited for Pacific herring to conclusively determine the effects of chronic elevated pCO_2 on exercise performance (Tudorache et al. 2013).

5. CONCLUSIONS

Our findings demonstrate that the growth, survival, and VHS susceptibility of young-of-the-year Pacific herring are not affected by pCO_2 concentrations that are expected to occur in the Salish Sea and surrounding coastal regions by the end of this century (i.e. <1500 µatm pCO_2). Furthermore, we show that key traits related to early larval development and juvenile growth are unaffected by extreme acidification up to 3000 µatm pCO_2. These results are consistent with the results of several studies focused on the early life stages of clupeids and other coastal fish species that are generally tolerant of elevated pCO_2. However, Pacific herring that were reared at 3000 µatm pCO_2 exhibited greater vulnerability to VHS through increased mortality and survivors of the virus were in poorer condition compared to conspecifics reared at 650 and 1500 µatm pCO_2. In this context, it is important to note that concentrations as high as 3000 µatm pCO_2 are unlikely to persist for extended periods in coastal ecosystems of the North Pacific and may only arise during brief extreme events. Our results suggest that early life stages of this important forage fish species are likely able to tolerate near-future ocean acidification conditions, at least with respect to the response variables we tested. The impacts of exposure to extreme acidification events could be prioritized for further research.

Data archive. All reported data sets are available at https://zenodo.org/doi/10.5281/zenodo.11473922.

Acknowledgements. Primary research funding and support for C.S.M. and T.K. was provided by the Washington Ocean Acidification Center. C.S.M. was supported by a National Science Foundational Postdoctoral Research Fellowship during manuscript preparation (Award Number 2126533). Matching support was provided by the *Exxon Valdez* Oil Spill Trustee Council (Project no. 21120111-E) and the U.S. Geological Survey, Ecosystems Mission Area, Biological Threats and Invasive Species Program Area. We are grateful to the Washington Department of Fish and Wildlife for providing wild herring embryos. We express our gratitude to David Paez for his valuable assistance with the statistical aspects of the survival analysis. We acknowledge Audrey Malloy (Western Washington University) for assisting with morphometric measurements and Willie Richards (U.S. Geological Survey) for assisting with fish care. We thank the Shannon Point Marine Center and Brooke Love for the use of their Seawater Chemistry Laboratory and other analytical instruments. Any use of trade, firm, or product names is for descriptive purposes only and does not imply endorsement by the U.S. Government.

LITERATURE CITED

Alter K, Peck MA (2021) Ocean acidification but not elevated spring warming threatens a European seas predator. Sci Total Environ 782:146926

Bates D, Mächler M, Bolker B, Walker S (2015) Fitting linear mixed-effects models using lme4. J Stat Softw 67:1–48

Batts WN, Winton JR (1989) Enhanced detection of infectious hematopoietic necrosis virus and other fish viruses by pretreatment of cell monolayers with polyethylene glycol. J Aquat Anim Health 1:284–290

Baumann H (2019) Experimental assessments of marine species sensitivities to ocean acidification and co-stressors: How far have we come? Can J Zool 97:399–408

Bednaršek N, Newton JA, Beck MW, Alin SR, Feely RA, Christman NR, Klinger T (2021) Severe biological effects under present-day estuarine acidification in the seasonally variable Salish Sea. Sci Total Environ 765: 142689

Brauner CJ, Shartau RB, Damsgaard C, Esbaugh AJ, Wilson RW, Grosell M (2019) Acid–base physiology and CO_2 homeostasis: regulation and compensation in response to elevated environmental CO_2. In: Grosell M, Munday PL, Farrell AP, Brauner CJ (eds) Fish physiology, Vol 37. Academic Press, New York, NY, p 69–132

Bresolin de Souza K, Asker N, Jönsson E, Förlin L, Sturve J (2016) Increased activity of lysozyme and complement system in Atlantic halibut exposed to elevated CO_2 at six different temperatures. Mar Environ Res 122:143–147

Brett JR (1964) The respiratory metabolism and swimming

performance of young sockeye salmon. J Fish Res Board Can 21:1183–1226

Burge CA, Hershberger PK (2020) Climate change can drive marine diseases. In: Behringer DC, Silliman BR, Lafferty KD (eds) Marine disease ecology. Oxford Academic, Oxford, p 83–94

Cai WJ, Feely RA, Testa JM, Li M and others (2021) Natural and anthropogenic drivers of acidification in large estuaries. Annu Rev Mar Sci 13:23–55

Cao R, Wang Q, Yang D, Liu Y and others (2018) CO_2-induced ocean acidification impairs the immune function of the Pacific oyster against *Vibrio splendidus* challenge: an integrated study from a cellular and proteomic perspective. Sci Total Environ 625:1574–1583

Cohen-Rengifo M, Danion M, Gonzalez AA, Bégout ML and others (2022) The extensive transgenerational transcriptomic effects of ocean acidification on the olfactory epithelium of a marine fish are associated with a better viral resistance. BMC Genomics 23:448

Cominassi L, Moyano M, Claireaux G, Howald S and others (2019) Combined effects of ocean acidification and temperature on larval and juvenile growth, development and swimming performance of European sea bass (*Dicentrarchus labrax*). PLOS ONE 14:e0221283

Dahlke F, Lucassen M, Bickmeyer U, Wohlrab S and others (2020) Fish embryo vulnerability to combined acidification and warming coincides with low capacity for homeostatic regulation. J Exp Biol 223:jeb.212589

Dickson AG (1990) Standard potential of the reaction: $AgCl(s) + 12H_2(g) = Ag(s) + HCl(aq)$, and the standard acidity constant of the ion HSO_4^- in synthetic sea water from 273.15 to 318.15 K. J Chem Thermodyn 22:113–127

Dickson AG (2024) Information on batches of CO_2 in seawater reference material. National Centers for Environmental Information, Boulder, CO

Dickson A, Millero F (1987) A comparison of the equilibrium constants for the dissociation of carbonic acid in seawater media. Deep-Sea Res A 34:1733–1743

Doney SC, Busch DS, Cooley SR, Kroeker KJ (2020) The impacts of ocean acidification on marine ecosystems and reliant human communities. Annu Rev Environ Resour 45:83–112

Downie AT, Illing B, Faria AM, Rummer JL (2020) Swimming performance of marine fish larvae: review of a universal trait under ecological and environmental pressure. Rev Fish Biol Fish 30:93–108

Dunkler D, Ploner M, Schemper M, Heinze G (2018) Weighted Cox regression using the R package coxphw. J Stat Softw 84:1–26

Escobar LE, Escobar-Dodero J, Phelps NBD (2018) Infectious disease in fish: global risk of viral hemorrhagic septicemia virus. Rev Fish Biol Fish 28:637–655

Evans W, Pocock K, Hare A, Weekes C and others (2019) Marine CO_2 patterns in the northern Salish Sea. Front Mar Sci 5:536

Farrell A (2008) Comparisons of swimming performance in rainbow trout using constant acceleration and critical swimming speed tests. J Fish Biol 72:693–710

Fassbender AJ, Alin SR, Feely RA, Sutton AJ and others (2018) Seasonal carbonate chemistry variability in marine surface waters of the US Pacific Northwest. Earth Syst Sci Data 10:1367–1401

Frommel AY, Maneja R, Lowe D, Malzahn AM and others (2012) Severe tissue damage in Atlantic cod larvae under increasing ocean acidification. Nat Clim Chang 2:42–46

Frommel AY, Maneja R, Lowe D, Pascoe CK and others (2014) Organ damage in Atlantic herring larvae as a result of ocean acidification. Ecol Appl 24:1131–1143

Frommel AY, Lye SLR, Brauner CJ, Hunt BPV (2022) Air exposure moderates ocean acidification effects during embryonic development of intertidally spawning fish. Sci Rep 12:12270

Gattuso JP, Epitalon JM, Lavigne H, Orr J (2020) seacarb: seawater carbonate chemistry. R package version 3.2.13. https://CRAN.R-project.org/package=seacarb

Hamilton TJ, Tresguerres M, Kwan GT, Szaskiewicz J and others (2023) Effects of ocean acidification on dopamine-mediated behavioral responses of a coral reef damselfish. Sci Total Environ 877:162860

Hansen JD, Woodson JC, Hershberger PK, Grady C, Gregg JL, Purcell MK (2012) Induction of anti-viral genes during acute infection with Viral hemorrhagic septicemia virus (VHSV) genogroup IVa in Pacific herring (*Clupea pallasii*). Fish Shellfish Immunol 32:259–267

Hershberger PK, Purcell MK, Hart LM, Gregg JL, Thompson RL, Garver KA, Winton JR (2013) Influence of temperature on viral hemorrhagic septicemia (Genogroup IVa) in Pacific herring, *Clupea pallasii* Valenciennes. J Exp Mar Biol Ecol 444:81–86

Hershberger PK, Garver KA, Winton JR (2016) Principles underlying the epizootiology of viral hemorrhagic septicemia in Pacific herring and other fishes throughout the North Pacific Ocean. Can J Fish Aquat Sci 73:853–859

Hershberger PK, MacKenzie AH, Gregg JL, Wilmot MD, Powers RL, Purcell MK (2021a) Long-term shedding from fully convalesced individuals indicates that Pacific herring are a reservoir for viral hemorrhagic septicemia virus. Dis Aquat Org 144:245–252

Hershberger PK, Meyers TR, Gregg JL, Groner ML and others (2021b) Annual recurrences of viral hemorrhagic septicemia epizootics in age 0 Pacific herring *Clupea pallasii* Valenciennes, 1847. Animals (Basel) 11:2426

Heuer RM, Hamilton TJ, Nilsson GE (2019) The physiology of behavioral impacts of high CO_2. In: Grosell M, Munday PL, Farrell AP, Brauner CJ (eds) Fish physiology, Vol 37. Academic Press, New York, NY, p 161–194

Hurst TP, Fernandez ER, Mathis JT, Miller JA, Stinson CM, Ahgeak EF (2012) Resiliency of juvenile walleye pollock to projected levels of ocean acidification. Aquat Biol 17: 247–259

Huth TJ, Place SP (2016) RNA-seq reveals a diminished acclimation response to the combined effects of ocean acidification and elevated seawater temperature in *Pagothenia borchgrevinki*. Mar Genomics 28:87–97

Ishimatsu A, Hayashi M, Kikkawa T (2008) Fishes in high-CO_2, acidified oceans. Mar Ecol Prog Ser 373:295–302

Jarrold MD, Munday PL (2018) Diel CO_2 cycles do not modify juvenile growth, survival and otolith development in two coral reef fish under ocean acidification. Mar Biol 165:49

Joly LJ, Boersma M, Giraldo C, Mazurais D and others (2023) Smaller herring larval size-at-stage in response to environmental changes is associated with ontogenic processes and stress response. Conserv Physiol 11:coad072

Kang J, Nagelkerken I, Rummer JL, Rodolfo-Metalpa R, Munday PL, Ravasi T, Schunter C (2022) Rapid evolution fuels transcriptional plasticity to ocean acidification. Glob Change Biol 28:3007–3022

Kawakami T, Okouchi H, Aritaki M, Aoyama J, Tsukamoto K (2011) Embryonic development and morphology of eggs

and newly hatched larvae of Pacific herring *Clupea pallasii*. Fish Sci 77:183–190
Kreiss CM, Michael K, Bock C, Lucassen M, Pörtner HO (2015) Impact of long-term moderate hypercapnia and elevated temperature on the energy budget of isolated gills of Atlantic cod (*Gadus morhua*). Comp Biochem Physiol A Mol Integr Physiol 182:102–112
Kunz KL, Claireaux G, Pörtner HO, Knust R, Mark FC (2018) Aerobic capacities and swimming performance of polar cod (*Boreogadus saida*) under ocean acidification and warming conditions. J Exp Biol 221:jeb184473
Kuznetsova A, Brockhoff PB, Christensen RHB (2017) lmerTest package: tests in linear mixed effects models. J Stat Softw 82:1–26
Kwan GT, Shen SG, Drawbridge M, Checkley DM, Tresguerres M (2021) Ion-transporting capacity and aerobic respiration of larval white seabass (*Atractoscion nobilis*) may be resilient to ocean acidification conditions. Sci Total Environ 791:148285
Lenth R (2018) emmeans: estimated marginal means, aka least-squares means. R package version 1.2.3. https://CRAN.R-project.org/package=emmeans
Liu S, Shi W, Guo C, Zhao X and others (2016) Ocean acidification weakens the immune response of blood clam through hampering the NF-kappa β and toll-like receptor pathways. Fish Shellfish Immunol 54:322–327
Lonthair J, Ern R, Esbaugh AJ (2017) The early life stages of an estuarine fish, the red drum (*Sciaenops ocellatus*), are tolerant to high pCO_2. ICES J Mar Sci 74:1042–1050
Love BA, Olson MB, Wuori T (2017) Technical note: a minimally invasive experimental system for pCO_2 manipulation in plankton cultures using passive gas exchange (atmospheric carbon control simulator). Biogeosciences 14:2675–2684
Lüdecke D, Makowski D, Waggoner P (2020) performance: assessment of regression models performance. R package version 0.4.8. https://CRAN.R-project.org/package=performance
Marty GD, Hulson PJF, Miller SE, Quinn TJ II, Moffitt SD, Merizon RA (2010) Failure of population recovery in relation to disease in Pacific herring. Dis Aquat Org 90:1–14
Mazurais D, Neven CJ, Servili A, Vitré T and others (2021) Effect of long-term intergenerational exposure to ocean acidification on *ompa* and *ompb* transcripts expression in European seabass (*Dicentrarchus labrax*). Mar Environ Res 170:105438
McLaskey AK, Keister JE, McElhany P, Olson MB, Busch DS, Maher M, Winans AK (2016) Development of *Euphausia pacifica* (krill) larvae is impaired under pCO_2 levels currently observed in the Northeast Pacific. Mar Ecol Prog Ser 555:65–78
Michael K, Kreiss CM, Hu MY, Koschnick N and others (2016) Adjustments of molecular key components of branchial ion and pH regulation in Atlantic cod (*Gadus morhua*) in response to ocean acidification and warming. Comp Biochem Physiol B Biochem Mol Biol 193:33–46
Mittermayer FH, Stiasny MH, Clemmesen C, Bayer T and others (2019) Transcriptome profiling reveals exposure to predicted end-of-century ocean acidification as a stealth stressor for Atlantic cod larvae. Sci Rep 9:16908
Munday PL (2014) Transgenerational acclimation of fishes to climate change and ocean acidification. F1000Prime Rep 6:99
Murray CS, Baumann H (2018) You better repeat it: complex CO_2 × temperature effects in Atlantic silverside offspring revealed by serial experimentation. Diversity (Basel) 10:69
Murray CS, Baumann H (2020) Are long-term growth responses to elevated pCO_2 sex-specific in fish? PLOS ONE 15:e0235817
Murray CS, Klinger T (2022) High pCO_2 does not alter the thermal plasticity of developing Pacific herring embryos during a marine heatwave. J Exp Biol 225:jeb243501
Murray CS, Malvezzi A, Gobler CJ, Baumann H (2014) Offspring sensitivity to ocean acidification changes seasonally in a coastal marine fish. Mar Ecol Prog Ser 504:1–11
Murray CS, Fuiman LA, Baumann H (2017) Consequences of elevated CO_2 exposure across multiple life stages in a coastal forage fish. ICES J Mar Sci 74:1051–1061
Murray CS, Wiley D, Baumann H (2019) High sensitivity of a keystone forage fish to elevated CO_2 and temperature. Conserv Physiol 7:coz084
Pacella SR, Brown CA, Waldbusser GG, Labiosa RG, Hales B (2018) Seagrass habitat metabolism increases short-term extremes and long-term offset of CO_2 under future ocean acidification. Proc Natl Acad Sci USA 115:3870–3875
Peake S, Farrell A (2006) Fatigue is a behavioural response in respirometer-confined smallmouth bass. J Fish Biol 68:1742–1755
Pechenik JA (2006) Larval experience and latent effects — metamorphosis is not a new beginning. Integr Comp Biol 46:323–333
Perry SF, Gilmour KM (2006) Acid–base balance and CO_2 excretion in fish: unanswered questions and emerging models. Respir Physiol Neurobiol 154:199–215
Philip SY, Kew SF, van Oldenborgh GJ, Anslow FS and others (2021) Rapid attribution analysis of the extraordinary heatwave on the Pacific Coast of the US and Canada June 2021. Earth Syst Dynam Discuss 2021:1–34
Rombough PJ (2006) Developmental costs and the partitioning of metabolic energy. In: Warburton SJ, Burggren WW, Pelster B, Reiber CL, Spicer J (eds) Comparative developmental physiology: contributions, tools and trends. Oxford University Press, New York, NY, p 99–123
Rueden CT, Schindelin J, Hiner MC, DeZonia BE, Walter AE, Arena ET, Eliceiri KW (2017) ImageJ2: ImageJ for the next generation of scientific image data. BMC Bioinformatics 18:529
Ruiz-Jarabo I, Gregório SF, Alves A, Mancera JM, Fuentes J (2021) Ocean acidification compromises energy management in *Sparus aurata* (Pisces: Teleostei). Comp Biochem Physiol A Mol Integr Physiol 256:110911
Sandell T, Lindquist A, Dionne P, Lowry D (2019) 2016 Washington State herring stock status report. Species Status Reports. Fish Program Technical Report No. FPT 19-07. Washington Department of Fish and Wildlife, Olympia, WA
Schemper M, Wakounig S, Heinze G (2009) The estimation of average hazard ratios by weighted Cox regression. Stat Med 28:2473–2489
Schunter C, Jarrold MD, Munday PL, Ravasi T (2021) Diel pCO_2 fluctuations alter the molecular response of coral reef fishes to ocean acidification conditions. Mol Ecol 30:5105–5118
Servili A, Lévêque E, Mouchel O, Devergne J and others (2023) Ocean acidification alters the acute stress response of a marine fish. Sci Total Environ 858:159804
Sewall F, Norcross B, Heintz R (2021) Growth, condition,

and swimming performance of juvenile Pacific herring with winter feeding rations. Can J Fish Aquat Sci 78: 881–893

Singh NR, Love B, Murray CS, Sobocinski KL, Cooper WJ (2023) The combined effects of acidification and acute warming on the embryos of Pacific herring (*Clupea pallasii*). Front Mar Sci 10:1307617

Sswat M, Stiasny MH, Jutfelt F, Riebesell U, Clemmesen C (2018) Growth performance and survival of larval Atlantic herring, under the combined effects of elevated temperatures and CO_2. PLOS ONE 13:e0191947

Stevenson JC (1962) Distribution and survival of herring larvae (*Clupea pallasi* Valenciennes) in British Columbia waters. J Fish Res Board Can 19:735–810

Stiasny MH, Mittermayer FH, Sswat M, Voss R and others (2016) Ocean acidification effects on Atlantic cod larval survival and recruitment to the fished population. PLOS ONE 11:e0155448

Sundin J, Amcoff M, Mateos-González F, Raby GD, Clark TD (2019) Long-term acclimation to near-future ocean acidification has negligible effects on energetic attributes in a juvenile coral reef fish. Oecologia 190:689–702

Surma S, Pitcher TJ, Pakhomov EA (2021) Trade-offs and uncertainties in Northeast Pacific herring fisheries: ecosystem modelling and management strategy evaluation. ICES J Mar Sci 78:2280–2297

Tangherlini M, Corinaldesi C, Ape F, Greco S, Romeo T, Andaloro F, Danovaro R (2021) Ocean acidification induces changes in virus–host relationships in Mediterranean benthic ecosystems. Microorganisms 9:769

Toy JA, Kroeker KJ, Logan CA, Takeshita Y, Longo GC, Bernardi G (2022) Upwelling-level acidification and pH/pCO_2 variability moderate effects of ocean acidification on brain gene expression in the temperate surfperch, *Embiotoca jacksoni*. Mol Ecol 31:4707–4725

Tracy AM, Pielmeier ML, Yoshioka RM, Heron SF, Harvell CD (2019) Increases and decreases in marine disease reports in an era of global change. Proc R Soc B 286: 20191718

Tudorache C, de Boeck G, Claireaux G (2013) Forced and preferred swimming speeds of fish: a methodological approach. In: Palstra AP, Planas JV (eds) Swimming physiology of fish: towards using exercise to farm a fit fish in sustainable aquaculture. Springer, Berlin Heidelberg, p 81–108

Villalobos C, Love BA, Olson MB (2020) Ocean acidification and ocean warming effects on Pacific herring (*Clupea pallasi*) early life stages. Front Mar Sci 7:597899

Vilmar M, Di Santo V (2022) Swimming performance of sharks and rays under climate change. Rev Fish Biol Fish 32:765–781

Warton DI, Hui FK (2011) The arcsine is asinine: the analysis of proportions in ecology. Ecology 92:3–10

Williams CR, Dittman AH, McElhany P, Busch DS and others (2019) Elevated CO_2 impairs olfactory-mediated neural and behavioral responses and gene expression in ocean-phase coho salmon (*Oncorhynchus kisutch*). Glob Change Biol 25:963–977

Wood S, Wood MS (2015) mgcv: Mixed GAM Computation Vehicle with automatic smoothness estimation. R package version 1.7-29. https://CRAN.R-project.org/package=mgcv

Zha S, Liu S, Su W, Shi W, Xiao G, Yan M, Liu G (2017) Laboratory simulation reveals significant impacts of ocean acidification on microbial community composition and host–pathogen interactions between the blood clam and *Vibrio harveyi*. Fish Shellfish Immunol 71:393–398

Editorial responsibility: Konstantinos Stergiou, Thessaloniki, Greece
Reviewed by: 2 anonymous referees

Submitted: November 14, 2023
Accepted: April 23, 2024
Proofs received from author(s): June 7, 2024